Simulation and Design of Ground-Penetrating Radar for Mars Exploration

C. J. Leuschen[1], S. P. Gogineni[1], S. M. Clifford[2], and R. K. Raney[3]
[1]RSL, The University of Kansas, 2335 Irving Hill Road, Lawrence, KS 66045
[2]LPI, 3600 Bay Area Boulevard, Houston, TX 77058
[3]APL, Johns Hopkins University, 11100 Johns Hopkins Road, Laurel, MD 20723
Phone: (785) 864-7739, Fax: (785) 864-7789, E-mail: leuschen@rsl.ukans.edu

Abstract - Over the past few years, the interest in exploring Mars has grown, with several missions in the planning stages for the next decade. One motivating theme is the potential of discovering substantial sub-surface aqueous reservoirs. This paper outlines the simulation and development of a lightweight, low-power, ground-penetrating radar system intended for the subsurface exploration of Mars.

I. INTRODUCTION

For many years man has been exploring Mars. The first historical study of Mars is credited to two sketches by Francisco Fontana that were rendered from his telescopic observations in 1638 [1]. From then on, many others have gathered information on this planet using telescopes, orbiting satellites, and more recently lander-based equipment. Around 1877, a map by Giovanni Virginio Schiaparelli described the popular “canali” or channels and consequently reinforced the idea that Mars may contain a significant amount of water.

There is evidence that Mars has undergone considerable geological change over its history, and that surface water played an important role in those changes. “Some researchers suggest that early Mars was warm and wet, and conditions changed early to the frigid conditions of today [2].” If discovered, the presence of water would be important for three major reasons. First, it could provide a better understanding of the geological history of the planet. Second, water is the key to life on Earth, and on Mars it could indicate the possibility of past life. Finally, any accessible reservoirs could provide crucial resources for future manned exploration.

This paper considers the simulation and design of a ground-penetrating radar (GPR) system to probe the Martian subsurface for aqueous layers in either liquid or solid state. Depth of a few hundred meters to as much as a kilometer are required, at a resolution of a few tens of meters. The geophysical objectives include surface characterization, determining soil properties at microwave frequencies, and three-dimensional stratigraphy mapping.

II. SIMULATION

An essential step in designing such a system is to simulate the radar responses from geophysical models based on what could be expected on Mars. The two boxes on the left-hand side of the simulation flow chart (Fig. 1) indicate all inputs for the simulation, including the geophysical model and system parameters. A GPR profile (wavenumber as a function of depth and frequency) is generated from the electrical properties and mixing formulas appropriate to the modeled stratigraphy. Finally, the profile along with additional system and ground information are input to the simulator and a radar response is generated.

A. Geophysical Model and Electrical Properties

“Stratigraphy forms the framework of historical geology [3].” It expresses the relationship of the rocks and soils of the terrain and the subsurface. From a radar perspective, the idea of stratigraphy changes from the distributions of the physical rocks and soils to the distribution of their electrical properties, especially permittivity and permeability. The upper surface of Mars is largely a result of resurfacing by volcanic, fluvial, aeolian, periglacial, and impact processes. It is estimated that this layer of displaced materials covers the planet with a two-kilometer blanket [4]. On a large scale, the stratigraphy of Mars can be interpreted as a weathered soil with an exponentially decaying porosity. Using lunar data as reference, we can assume that porosity at the surface varies from 20 to 50 percent, and the decay constant can be estimated to be 2.8. Within the pores of this soil could exist a significant amount of water as ice near the surface and as liquid at greater depths. On a smaller scale, “it is likely that this ejecta (resurfaced) layer is discontinuously interbedded with volcanic flows, weathering products, and sedimentary deposits, all overlying a heavily fractured basement [4]”.

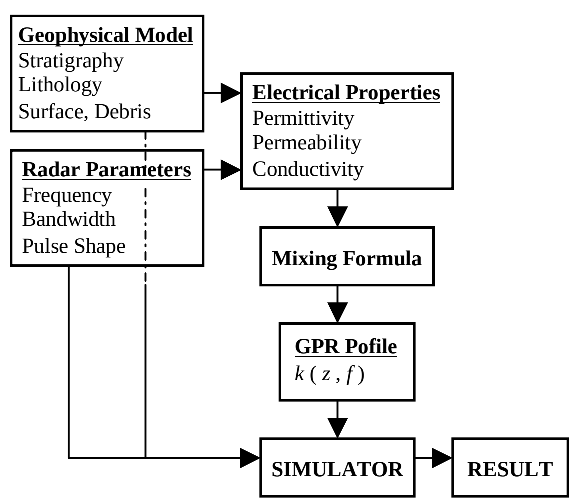

Fig. 1. Simulation flow chart.

0-7803-7033-3/01/$10.00 (C) 2001 IEEE

The surface and subsurface layers of Mars will exhibit both large and small scales of roughness. Each height scale can be described by a Gaussian random variable with r.m.s. height, σ, correlation length, l, and r.m.s. slope, s, where $s^2 = 2\sigma^2/l^2$. The large-scale r.m.s. slope for the surface of Mars is expected to be less than 0.02 radians [5]. To an orbiting radar, the major contribution will be due to the large scale of roughness at small incident angles, which can be represented by the geometric-optics approximation for the backscattering coefficient [6].

$$\sigma^0(\theta) = \frac{|\Gamma|^2 \exp\left(-\tan^2\theta / 2s^2\right)}{2s^2 \cos^4\theta} \tag{1}$$

If the soil is interbedded with rocks and debris, an effective permittivity is used to account for the change in dielectric constant and attenuation due to scattering. For spherical inclusions of permittivity, ε_s, radius, a, and volume fraction, f_v, present in a background medium, ε_b, the effective permittivity is expressed by [7] as

$$\varepsilon_{eff} = \varepsilon \left\{ \begin{array}{l} \left[\dfrac{1+2 f_v (\varepsilon_s-\varepsilon_b)/(\varepsilon_s+2\varepsilon_b)}{1- f_v (\varepsilon_s-\varepsilon_b)/(\varepsilon_s+2\varepsilon_b)} \right] \\ -j 2 f_v k^3 a^3 \left| \dfrac{(\varepsilon_s-\varepsilon_b)/(\varepsilon_s+2\varepsilon_b)}{1- f_v (\varepsilon_s-\varepsilon_b)/(\varepsilon_s+2\varepsilon_b)} \right|^2 \dfrac{(1-f_v)^4}{(1+2 f_v)^2} \end{array} \right\}. \tag{2}$$

For the rocky surface of Mars, the size and distribution of rocks is estimated to be 1 centimeter to 7 meters and less than a 30 percent volume fraction. These properties are assumed to be indicative of the near-subsurface characteristics.

The primary resources for estimating the electrical surface properties (complex permittivity and permeability) include surface measurements from the Viking Landers and Pathfinder Mission, analogies to lunar samples, SNC (Shergotty, Nakhla, Chassigny) meteorites, and interpretations from visible images. An exhaustive search of these resources indicates that the dielectric constant (real part of the permittivity) varies from 2.5 to 9 depending on the porosity of the medium. However, there is little information on the permeability and electrical losses of the soil. For a water/ice/soil mixture, as shown in Fig. 2, the complex permittivity is obtained using equations in Table 1.

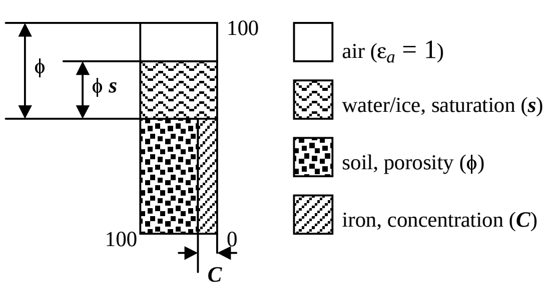

Fig. 2. Soil model.

B. One-Dimensional Simulations

For an orbit-based GPR, where the height of the radar is much greater than the depth of penetration, the transmission and reflection of the incident pulse can be approximated as a plane wave propagating through a layered media. This one-dimensional response is calculated by representing the subsurface as a set of transmission lines, each with a complex propagation constant and characteristic impedance, and calculating the complex reflection coefficient versus frequency. Corrections to spherical spreading and other system parameters are then made to the computed response. Table 2 shows the stratigraphy, lithology and resulting complex permittivity for a model of an equatorial site. A 10 MHz center frequency, 5 MHz bandwidth, modulated Gaussian pulse is used as the incident waveform. The results of the one-dimensional simulation are shown in Fig 3.

C. Three-Dimensional Simulation

Due to the nature of rough surface scattering, the radar return can be well simulated only if the backscatter from off-nadir incident angles is included. By doing so, the off-nadir clutter can mask deeper responses.

The simulated three-dimensional response is calculated using these steps:

1) Generating the one-dimensional plane wave response.
2) Multiplying by the antenna pattern and surface backscatter and time scaling for responses from off-nadir angles.
3) Convolving with a surface random variable.
4) Applying spherical spreading loss and other system parameters.

The three-dimensional radar response for the first model is also shown in Fig 3. when a 0.01 radian r.m.s. surface slope is considered.

TABLE 1
SOIL ELECTRICAL PROPERTIES

Material	**Properties [8]-[9]:** $\varepsilon_r = \varepsilon_r' - j\varepsilon_r''$, $\delta = \varepsilon_r''/\varepsilon_r'$
water/ice	$\varepsilon_w = \varepsilon_\infty + \dfrac{\varepsilon_s - \varepsilon_\infty}{1+j\omega\tau} - j\dfrac{\sigma}{\varepsilon_0\omega}$
soil: **linear mixing**	$\varepsilon_r = 4.7 - j0.0$
geometric mixing	$\varepsilon_s' = 9.0$ $\delta_s = (1.75 + 82.5C)10^{-3}$
mixing formulas: **linear mean**	$\varepsilon_m = \phi(1-s)\varepsilon_a + (\phi s)\varepsilon_w + (1-\phi)\varepsilon_s$
geometric mean	$\varepsilon_m = \varepsilon_a^{\phi(1-s)} \varepsilon_w^{\phi s} \varepsilon_s^{(1-\phi)}$

TABLE 2
SIMULATION MODEL
IRON CONCENTRATION C = 10% , VOLUME DEBRIS a=1meter, *fv* = 10%

depth	lithology	ϕ%	s%	fill	ε_r'	ε_r''
400km	air	100	-	-	-	-
1	eolian sediment	50	0	air	2.8	0.01
3	indurated sediment	15	0	air	5.9	0.05
5	sediment-filled basalt	50	0	air	2.8	0.01
10	dense basalt	5	0	air	7.2	0.07
100	layered basalt	10	0	air	6.4	0.06
110	eolian sediment	50	100	ice	5.1	0.04
150	layered basalt	10	50	ice	6.9	0.06
152	fluvial sediment	20	0	air	5.3	0.04
160	volcanic ash	50	0	air	2.8	0.01
200	layered basalt	10	0	air	6.5	0.06
220	crater ejecta	20	100	ice	6.7	0.06
250	layered basalt	10	100	ice	7.3	0.07
255	eolian sediment	50	0	air	2.8	0.01
350	layered basalt	10	0	air	6.5	0.06
355	fluvial sediment	20	0	air	5.3	0.04
500	layered basalt	10	0	air	6.5	0.06
750	layered basalt	10	100	ice	7.3	0.07
760	volcanic ash	50	100	ice	5.1	0.04
900	layered basalt	10	100	ice	7.3	0.07
1000	layered basalt	10	100	ice	7.3	0.07

The first layer represents the height of the radar.

IV. CONCLUSION AND FUTURE WORK

Fig. 3 shows the radar return for the two cases when a specular reflection and a rough surface response are considered for a multiple layer model. The specular, one-dimensional response can be viewed as the ideal or upper bound for the radar return, whereas the rough surface response shows a more realistic situation. Noise calculations show the minimum detectable signal to be approximately –140 dB. Using this minimal detectable signal level, this model would show a maximum penetration depth of about 400 meters.

The model presented in this paper represents only one example of what could be encountered. The penetration depth of a GPR on Mars is highly dependent on the stratigraphy and lithology of the subsurface layers. Since the electrical properties governing scattering and propagation of these layers are, to a large extent, unknown, predicting the performance of a radar is complicated and will involve extensive simulations over a wide range of models from simple two- to three- layer configurations to many-layer configurations of different geological locations.

For preliminary tests, a simple GPR system was constructed using evaluation boards and connectorized components to serve as a testbed for antenna design and field experiments. Some preliminary experiments have been completed on campus using 10 to 100 MHz bowtie antennas. More experiments are planned in Lawrence, KS and also in Alaska. Results from these experiments will be presented.

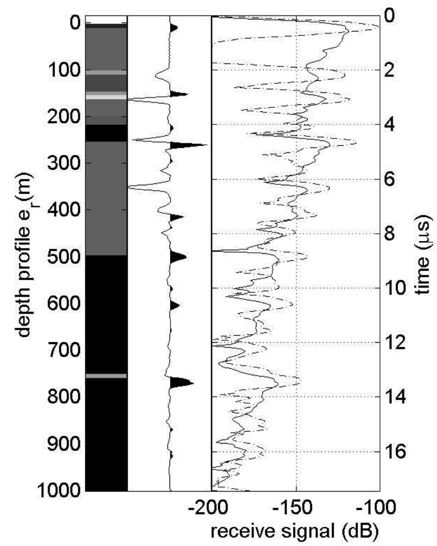

Fig 3. Simulation results. From left to right are the permittivity profile, one-dimensional amplitude response with a quadratic gain, dB plots normalized to the transmit signal for one (dashed) and three (solid) dimensional simulations.

REFERENCES

[1] H. H. Kieffer, B. M. Jakosky, and C. W. Snyder, “The Planet Mars: From Antiquity to the Present,” in *Mars*, H. H. Kieffer et al., Eds. Tuscon: University of Arizona, pp. 1-33, 1992.

[2] M. H. Carr, *Water on Mars*, New York: Oxford University, 1996.

[3] K. L. Tanaka, D. H. Scott, and R. Greenley, “Global Stratigraphy,” in *Mars*, H. H. Kieffer et al., Eds. Tuscon: University of Arizona, pp. 345-382, 1992.

[4] S. W. Squyres, S. M. Clifford, R. O. Kuzmin, J. R. Zimbelman, and F. M. Costard, “Ice in the Martian Regolith,” in *Mars*, H. H. Kieffer et al., Eds. Tuscon: University of Arizona, pp. 557-593, 1992.

[6] G. Picardi et al., “The Mars Advanced Radar for Subsurface and Ionosphere Sounding (MARSIS): concept and performance,” *Proceedings of the IEEE International Geoscience and Remote Sensing Symposium*, Hamburg, Germany, pp. 2674-2677, 1999.

[5] F.T. Ulaby, R.K. Moore, and A.K. Fung, *Microwave Remote Sensing Active and Passive: Vol. 2 Radar Remote Sensing and Surface Scattering and Emission Theory*, Norwood, MA: Artech House, 1982.

[7] J.A. Kong, *Electromagnetic Wave Theory*, New York: John Wiley and Sons, 1986.

[8] G.R.Olhoeft, “Electrical Properties of Rocks,” *Physical Properties of Rocks and Minerals*, Y. S. Touloukian, W.R. Judd, and R.F. Roy, Eds. New York: Hemisphere, pp. 257-330, 1989.

[9] F.T. Ulaby, R.K. Moore, and A.K. Fung, *Microwave Remote Sensing Active and Passive: Vol. 3 From Theory to Applications*, Norwood, MA: Artech House, 1986.